WORLD METEOROLOGICAL ORGANIZATION

GLOBAL ATMOSPHERE WATCH

WMO GREENHOUSE GAS BULLETIN

The State of Greenhouse Gases in the Atmosphere Based on Global Observations through 2022

No. 19 | 15 November 2023

ISSN 2078-0796

Achieving the goal of net-zero emissions and meeting the Paris Agreement's target of limiting global warming to well below 2 °C, with a specific focus on keeping it within 1.5 °C above the pre-industrial level, involves navigating numerous uncertainties. These uncertainties stem from scientific, technological, economic, social, and political complexities associated with global climate change. A growing body of literature highlights the following challenges in addressing the drivers of climate change, greenhouse gases (GHGs):

- **Feedback mechanisms**: The Earth's climate system has multiple feedback loops, including increased carbon emissions from soils and reduced carbon uptake by the oceans and forests due to the changing climate, as illustrated in a recent Nature Communications article concerning the droughts in Europe in 2018 and 2022 (see Figure 1(b)) [1];

- **Tipping points:** The climate system may be on the brink of "tipping points", critical thresholds where a certain degree of change triggers self-accelerating and potentially irreversible cascades of changes. Examples include the potential rapid die-back of the Amazon rainforest, the slowing of the North Atlantic circulation and the destabilization of large ice sheets;

- **Natural variability:** The three major greenhouse gases (GHGs): carbon dioxide (CO_2), methane (CH_4) and nitrous oxide (N_2O), have substantial variability driven by natural processes (for example, El Niño)

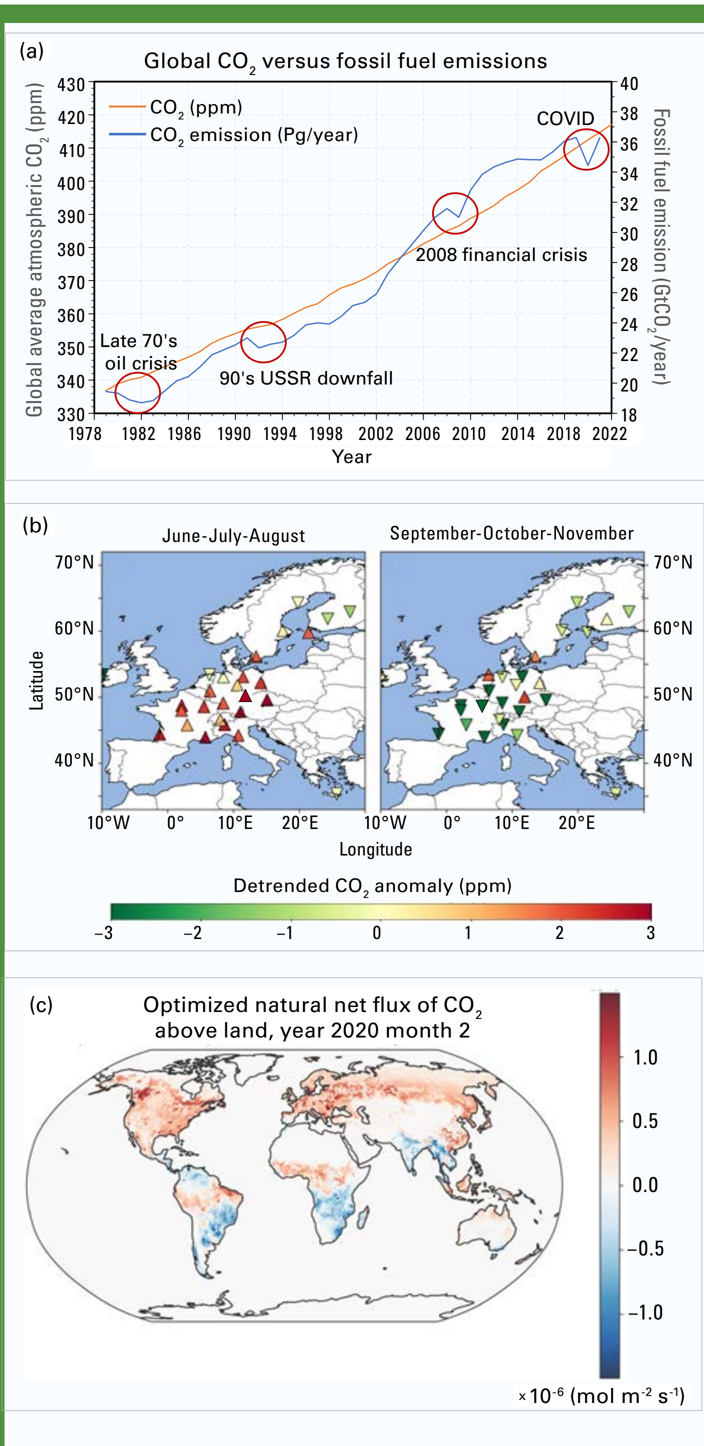

Figure 1. (a) Traditional annual global averages calculated with a delay of one year or more produced by the Global Carbon Project (GCP) for emissions and the GHG Bulletin for concentrations [2, 3]; (b) Current regional and spatially explicit analyses produced with a delay of a few months [1]. The map shows atmospheric CO_2 anomalies for June-July-August and September-October-November 2022 relative to 2019–2021. The red triangles show positive anomalies (less uptake), and the green triangles show negative anomalies (more uptake); (c) Monthly analyses produced by the NOAA CarbonTracker [4], currently with a delay of more than a year, globally and at high resolution. It is the goal of Global Greenhouse Gas Watch (GGGW) to produce internationally coordinated analyses like the one from NOAA but with monthly data at high spatial resolution and with a minimal delay incorporating, and extending, the existing data and modelling capacities of regional and national entities.

superimposed on anthropogenic signals. This variability can either amplify or dampen observed changes over short time frames;

- **Non-CO_2 greenhouse gases**: Climate change is driven by the presence of multiple greenhouse gases, not only CO_2. These gases have unique atmospheric lifetimes, greater Global Warming Potential (GWP) than CO_2 and uncertain future emission trends.

While the scientific community has a broad understanding of climate change and its implications, nuances and uncertainties persist. These uncertainties must not deter action. Rather, they underscore the need for flexible, adaptive strategies and the importance of risk management in the path to net-zero and the realization of the goals of the Paris Agreement. The provision of accurate, timely, and actionable data on GHG fluxes is vital. A routine and sustained global GHG monitoring system that utilizes numerous observations and modelling is needed to support ambitious climate goals. This new operational system will enhance the precision, sustainability and spatial coverage of existing measurement and modelling efforts, offering near-real-time, consistent data about GHG concentrations and fluxes. It will provide detailed information that is far beyond the annual global average and regional concentrations presented in this GHG Bulletin and GHG budgets estimated by the Global Carbon Project analyses.

Ensuring that GHG observations provide an accurate representation of the greenhouse gas balance within an operational GHG monitoring framework is a multifaceted challenge requiring a combination of technological, methodological, and collaborative approaches. In June 2023, the World Meteorological Congress, at its nineteenth session, adopted the Global Greenhouse Gas Watch (GGGW), detailed in the central insert of this issue, with the goal of providing, by 2028, with minimal delay and on a routine basis, monthly net GHG flux information at a grid of 1 degree by 1 degree for the entire world.

Current coordination efforts allow us to produce a global average CO_2 concentration, as illustrated in Figure 1(a). This global average number is minimally sensitive to changes in global emissions due to the long lifetime of CO_2 in the atmosphere. Figure 1(b) shows current regional and spatial analyses produced with a delay of several months developed by a regional monitoring infrastructure (the Integrated Carbon Observation System (ICOS)). These analyses provide more detailed information about CO_2 variations in the atmosphere in response to natural and anthropogenic factors. Figure 1(c) represents the global analysis of monthly CO_2 fluxes developed by a national institution (the National Oceanic and Atmospheric Administration (NOAA)). GGGW will build on the regional and national analyses illustrated in Figure 1(b) and 1(c) to establish an internationally coordinated GHG monitoring system.

Executive summary

The latest analysis of observations from the WMO Global Atmosphere Watch (GAW) in situ observational network shows that the globally averaged surface concentrations[(1)] for carbon dioxide (CO_2), methane (CH_4) and nitrous oxide (N_2O) reached new highs in 2022, with CO_2 at 417.9±0.2 ppm[(2)], CH_4 at 1923±2 ppb[(3)] and N_2O at 335.8±0.1 ppb. These values constitute, respectively, increases of 150%, 264% and 124% relative to pre-industrial (before 1750) levels. The increase in CO_2 from 2021 to 2022 was slightly lower than the increase observed from 2020 to 2021 and slightly lower than the average annual growth rate over the last decade; this was most likely partly caused by natural variability, as CO_2 emissions have continued to increase. For CH_4, the increase from 2021 to 2022 was slightly lower than that observed from 2020 to 2021 but considerably higher than the average annual growth rate over the last decade. For N_2O, the increase from 2021 to 2022 was higher than that observed any time before in our modern time record. The National Oceanic and Atmospheric Administration (NOAA) Annual Greenhouse Gas Index (AGGI) [5] shows that from 1990 to 2022, radiative forcing by long-lived greenhouse gases (LLGHGs) increased by 49%, with CO_2 accounting for about 78% of this increase.

Overview of observations from the GAW in situ observational network for 2022

This nineteenth annual WMO Greenhouse Gas Bulletin reports atmospheric abundances and rates of change of the most important LLGHGs – carbon dioxide, methane, and nitrous oxide – and provides a summary of the contributions of other greenhouse gases (GHGs). CO_2, CH_4 and N_2O, together with dichlorodifluoromethane (CFC-12) and trichlorofluoromethane (CFC-11), account for approximately 96%[(4)] [5] of radiative forcing due to LLGHGs (Figure 2).

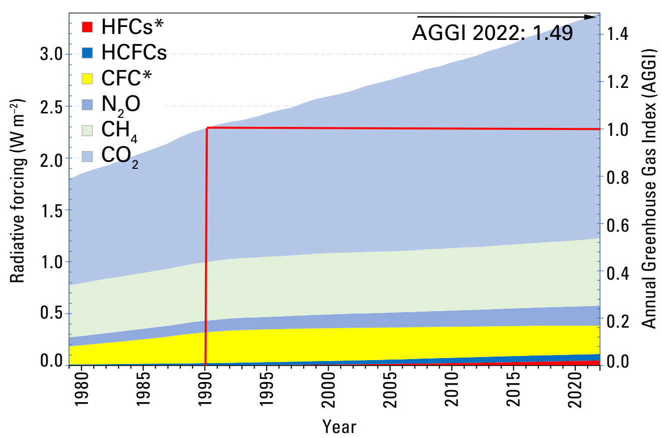

Figure 2. Atmospheric radiative forcing, relative to 1990, by LLGHGs corresponding to the 2022 update of the NOAA AGGI [5]

The WMO Global Atmosphere Watch Programme coordinates systematic observations and analyses of GHGs and other trace species. Sites where GHGs have been measured in the last decade are shown in Figure 3. Measurement data are reported by participating countries and archived and distributed by the WMO World Data Centre for Greenhouse Gases (WDCGG) at the Japan Meteorological Agency.

The results reported here by WMO WDCGG for the global average and growth rate are slightly different from the results reported by NOAA for the same years [6] due to differences in the stations used and the averaging procedure, as well as a slight difference in the time period for which the numbers are representative. WMO WDCGG follows the procedure described in detail in GAW Report No. 184 [7] and in [2]. The results reported here for CO_2 differ slightly from those in GHG Bulletins before 2020 (by approximately 0.2 ppm) because data are now reported on the new WMO CO_2 X2019 CO_2 calibration scale [8]. Historical data have been converted to the new scale to ensure consistency in reported trends.

The table provides globally averaged atmospheric abundances of the three major LLGHGs in 2022 and changes in their abundances since 2021 and 1750.

The three GHGs shown in the table are closely linked to anthropogenic activities and interact strongly with the biosphere and the oceans. Predicting the evolution of the atmospheric content of GHGs requires a quantitative understanding of their many sources, sinks and chemical transformations in the atmosphere. Observations from GAW provide invaluable constraints on the budgets of these and other LLGHGs and are used to improve emission estimates and evaluate satellite retrievals of LLGHG column averages. The Integrated Global Greenhouse Gas Information System (IG³IS) provides further insights on the sources of GHGs at the national and sub-national, especially urban, levels.

Table. Global annual surface mean abundances (2022) and trends of key greenhouse gases from the GAW in situ observational network for GHGs. The units are concentrations, and the uncertainties are 68% confidence limits. The averaging method is described in GAW Report No. 184 [7].

	CO_2	CH_4	N_2O
2022 global mean abundance	417.9±0.2 ppm	1923±2 ppb	335.8±0.1 ppb
2022 abundance relative to 1750[a]	150%	264%	124%
2021–2022 absolute increase	2.2 ppm	16 ppb	1.4 ppb
2021–2022 relative increase	0.53%	0.84%	0.42%
Mean annual absolute increase over the past 10 years	2.46 ppm yr^{-1}	10.2 ppb yr^{-1}	1.05 ppb yr^{-1}

[a] Assuming a pre-industrial concentration of 278.3 ppm for CO_2, 729.2 ppb for CH_4 and 270.1 ppb for N_2O. The number of stations used for the analyses was 146 for CO_2, 151 for CH_4 and 109 for N_2O.

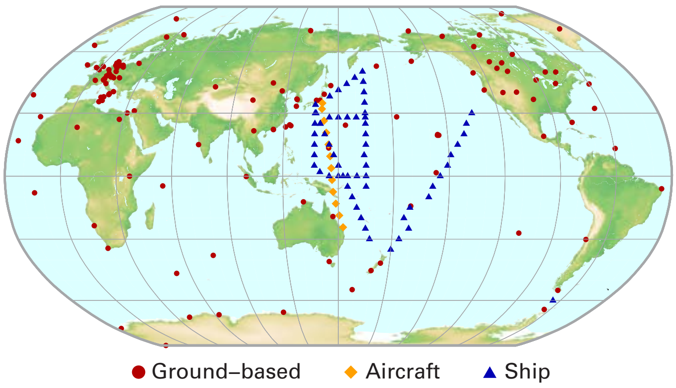

Figure 3. The GAW global network for CO_2 in the last decade. The network for CH_4 is similar. The in situ network for N_2O and other LLGHGs is far less dense.

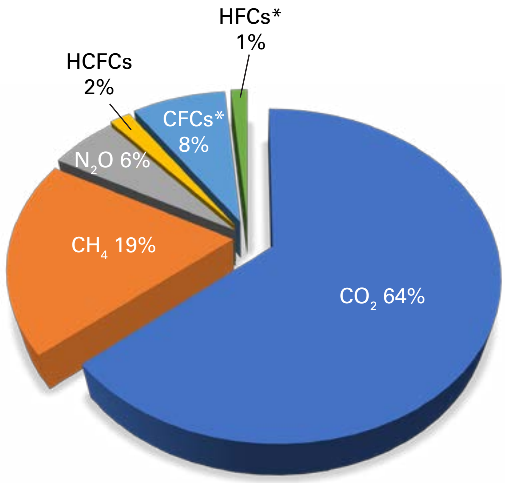

Figure 4. Contribution of the most important long-lived greenhouse gases to the increase in global radiative forcing from the pre-industrial era to 2022 [5].

The NOAA AGGI measures the increase in total radiative forcing due to all LLGHGs since 1990 [5]. The AGGI reached 1.49 in 2022, which represents a 49% increase in total radiative forcing from 1990 to 2022 and a 1.8% increase from 2021 to 2022 (Figure 2). The total radiative forcing by all LLGHGs in 2022 (3.398 W·m^{-2}) corresponds to an equivalent CO_2 concentraion of 523 ppm [5]. The relative contributions of various GHGs to the total radiative forcing since the pre-industrial era are presented in Figure 4.

Carbon dioxide (CO_2)

Carbon dioxide is the single most important anthropogenic greenhouse gas in the atmosphere, accounting for approximately 64%[4] of the radiative forcing by LLGHGs. It is responsible for about 79%[4] of the increase in radiative forcing over the past decade and about 77% of the increase over the past five years. The pre-industrial level of 278.3 ppm represented a balance of fluxes among the atmosphere, the oceans and the land biosphere. The globally averaged CO_2 concentration in 2022 was 417.9±0.2 ppm (Figure 5). The increase in annual means from 2021 to 2022, 2.2 ppm, was slightly smaller than the 2.5 ppm increase from 2020 to 2021 and slightly smaller than the average growth rate for the past decade (2.46 ppm yr^{-1}). There is no indication that the slower growth rate is due to decreasing fossil fuel emissions; instead, the most likely reason is the increased absorption of atmospheric CO_2 by terrestrial ecosystems and the oceans after several years with a La Niña (see WMO Greenhouse Gas Bulletin No. 12). The scientific consensus is that variability in the atmospheric CO_2 growth rate (Figure 5(b)) arises mainly from changing amounts of net CO_2 absorption by terrestrial ecosystems.

Atmospheric CO_2 reached 150% of the pre-industrial level in 2022, primarily because of emissions from the combustion of fossil fuels and cement production. According to the International Energy Agency (IEA), fossil fuel CO_2 emissions were projected to be 36.8 billion tons (Pg or Gt(5)) of CO_2 in 2022, up 0.8% from 36.5 Gt CO_2 in 2021 [9]. According to the 2022 analysis of the Global Carbon Project, deforestation and other land-use change contributed 4.5 (±2.6) Gt CO_2 yr^{-1}, on average, for the 2012–2021 period. Of the total emissions from human activities during the 2012–2021 period, about 48% accumulated in the atmosphere, 26% in the ocean and 29% on land, with the unattributed budget imbalance being 3% [3]. The portion of CO_2 emitted by fossil fuel combustion that remains in the atmosphere (airborne fraction (AF)), varies inter-annually due to the high natural variability of (mainly terrestrial) CO_2 sinks, although there is little evidence for a long-term AF trend (see also the cover story in WMO Greenhouse Gas Bulletin No. 17).

Methane (CH_4)

Methane accounts for about 19%(4) of the radiative forcing by LLGHGs. Approximately 40% of methane is emitted into the atmosphere by natural sources (for example, wetlands and termites), and about 60% comes from anthropogenic sources (for example, ruminants, rice agriculture, fossil fuel exploitation, landfills and biomass burning) [10]. The globally averaged CH_4 concentration calculated from in situ observations reached a new high of 1923 ± 2 ppb in 2022, an increase of 16 ppb with respect to the previous year (Figure 6). This increase is slightly lower than the increase of 17 ppb from 2020

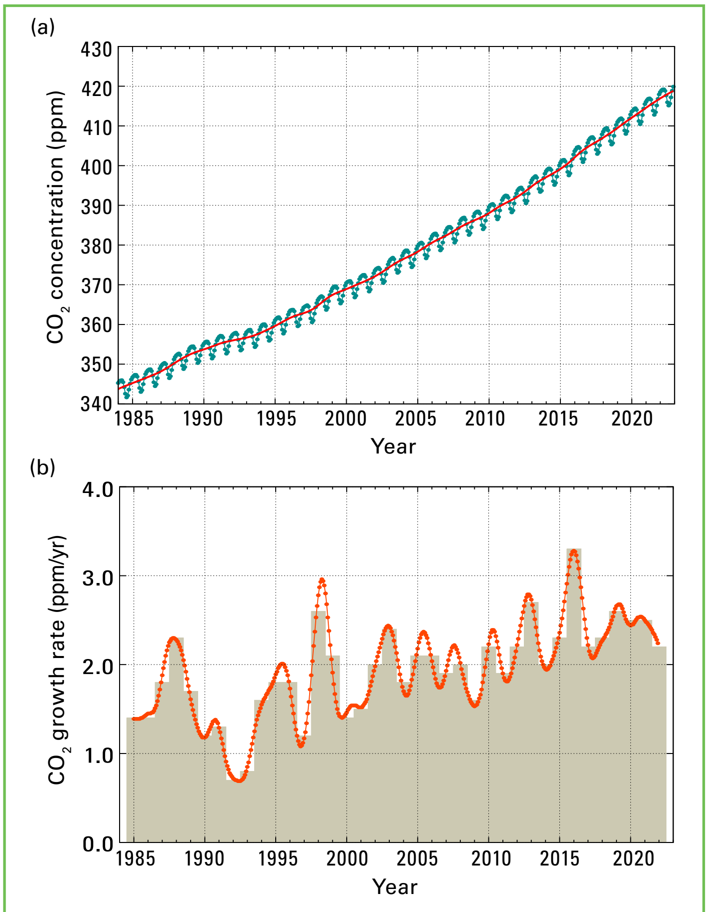

Figure 5. Globally averaged CO_2 concentration(1) (a) and its growth rate (b) from 1984 to 2022. Increases in successive annual means are shown as the shaded columns in (b). The red line in (a) is the monthly mean with the seasonal variation removed; the blue dots and blue line in (a) depict the monthly averages. Observations from 146 stations were used for this analysis.

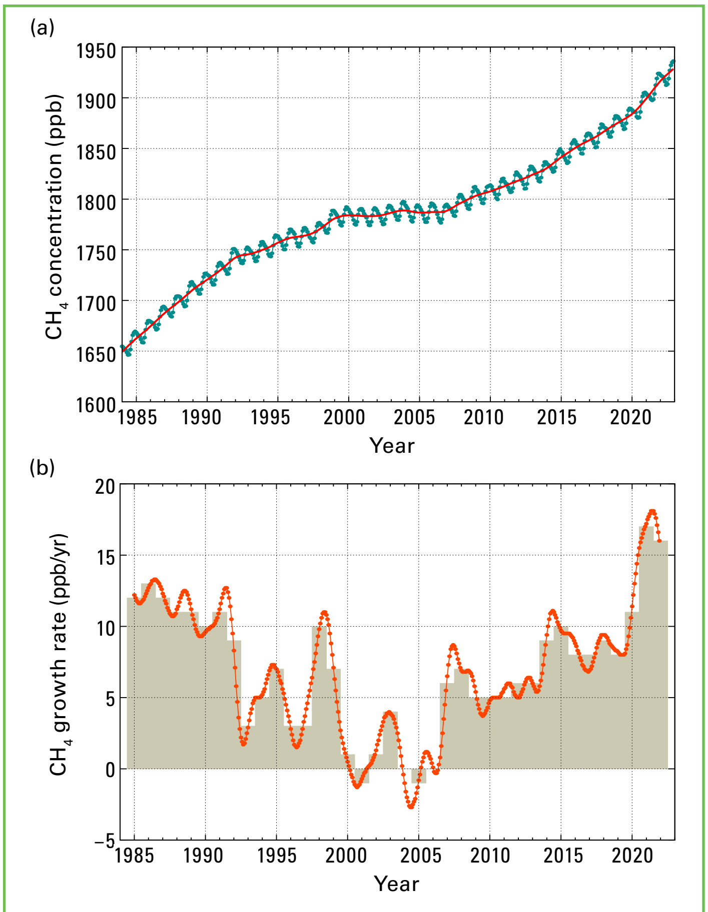

Figure 6. Globally averaged CH_4 concentration (a) and its growth rate (b) from 1984 to 2022. Increases in successive annual means are shown as the shaded columns in (b). The red line in (a) is the monthly mean with the seasonal variation removed; the blue dots and blue line in (a) depict the monthly averages. Observations from 151 stations were used for this analysis.

GLOBAL GREENHOUSE GAS WATCH

As shown in the cover story, the need for sustained and current data on greenhouse gases has become more acute. At the twenty-seventh Conference of the Parties to the United Nations Framework Convention on Climate Change in 2022, the Parties emphasized "the need to enhance coordination of activities by the systematic observation community and the ability to provide useful and actionable climate information for mitigation, adaptation and early warning systems".

In response to this need, WMO initiated the development of the Global Greenhouse Gas Watch (GGGW) (see https://www.gggw.earth), based on established methodologies and standardized protocols developed by the WMO GAW GHG community. GGGW will consolidate existing measurement and modelling capabilities and expand these capabilities where needed to provide estimates of total net GHG fluxes on a global scale at unprecedented high resolution in space and time. The initial outputs will include monthly CO_2 and CH_4 net fluxes between the surface of the Earth and the atmosphere with 1 degree x 1 degree horizontal resolution, delivered with a maximum delay of one month, and three-dimensional data-constrained fields of CO_2 and CH_4 abundance with hourly resolution and data latency on the order of a few days. This will lead to improved understanding of the fluxes and allow for better tracking and prediction of long-term future climate trajectories, with potentially strong implications for the required mitigation activities or planning of adaptation measures. The aim for the development of GGGW is that in 2028, each individual modelling system that is part of GGGW will deliver the outputs specified above in common standard formats.

In its initial configuration, GGGW will focus on the three major greenhouse gases contributing to human induced global warming: CO_2, CH_4, and N_2O. It will consist of four main components:

- A comprehensive sustained, global set of surface-based and satellite-based observations[1] of CO_2, CH_4 and N_2O concentrations, total column amounts, partial column amounts, vertical profiles, and fluxes, together with the supporting meteorological, oceanic, and terrestrial variables. The information will be exchanged in an open and transparent manner with minimum delay;
- Prior estimates of GHG sources and sinks based on activity data and process-based models;
- A set of global high-resolution Earth System models representing GHG cycles;
- Associated data assimilation systems that optimally combine observations with atmospheric transport model calculations to generate products of higher accuracy.

Efforts are underway to develop capabilities to further separate these net fluxes into source-apportioned emissions, which would lead to additional operational products in the future. Improved performance is expected as both observing and modelling capabilities improve. Many sources of uncertainty need to be overcome, including those related to the representation of atmospheric transport (both horizontal and vertical) in the models, the quality of the prior information and the limitations of the global observing system.

Defining the needs for the GGGW observation system, such as the required precision of the measurements and the spatial density of the ground-based observations, is under active discussion and depends on what the atmospheric transport models that will be used in the flux calculations can represent. Current global (inverse) models, for example some of those used in the Global Carbon Project, have lower resolutions than the goal of GGGW.

Atmospheric inversions deliver optimized fluxes and can provide information on how the assumed uncertainties in these fluxes was reduced by including information from the observations. This is usually expressed as a percentage of the original assumed uncertainty. When the uncertainty reduction is low, for example, one or two per cent, this tells us that we are missing information because there are not enough observations, or they are too far away, not precise enough (according to the specifications of the WMO GAW compatibility goals for surface-based observations [13]) or may provide conflicting information within the context of imperfection in the transport or priors. The reduction of uncertainty ideally should be as close as possible to 100%. The uncertainties of the initial flux estimates are not easy to quantify as many factors that contribute are not well known.

[1] In keeping with standard WMO terminology, the term "surface-based observing systems" (or networks) refers to any systems that are not deployed in space; the measurements may be in situ or remotely sensed, and they may pertain to any part of the Earth System domain (atmosphere, ocean, land, cryosphere, and so forth) and to any vertical level within the respective domain.

Figures 9 and 10 show the optimized terrestrial biogenic fluxes and the optimized air-sea fluxes for one particular advanced global inversion system, the European Copernicus CAMS system (resolution 1.2 degrees x 2.5 degrees), [14] based on the assimilation of two observational data sets, one from a satellite (OCO-2, which requires sunlight reflected from the surface) and one using surface-based observations. The upper panels show fluxes derived from inversions using satellite data, and the lower panels show fluxes derived from surface-based observations. The results are shown for January and July 2022. The matching uncertainty reductions are shown in the panels on the right. For January, the satellite observations lead to relatively small error reductions in the northern hemisphere (NH), but relatively high error reductions in the southern hemisphere (SH) above the continents. In contrast, surface-based observations lead to relatively high reductions in the NH above land and in parts of the Arctic Ocean and lower reductions in the SH (where surface observations are severely lacking), with the exception of the Southern Ocean where a few GAW background stations deliver data. In general, for both satellite and surface in situ data inversions, uncertainty reduction is driven by data density. For July 2022, the satellite information leads to relatively high uncertainty reductions over most continental areas, except North Africa. The uncertainty reduction from surface observations is in general higher for July compared to January, but in July, the reductions over the SH are smaller, especially over the oceans.

From these results, it is clear that surface and satellite data deliver complementary information. Inversions for regions are more uncertain when observations are missing. The current inversion results (at 2 degrees by 3 degrees horizontally, or even coarser) clearly indicate where we should enhance surface-based and space-based observations. By comparing different inversion systems that use different observation constellations, inversion methods, transport models and initial flux

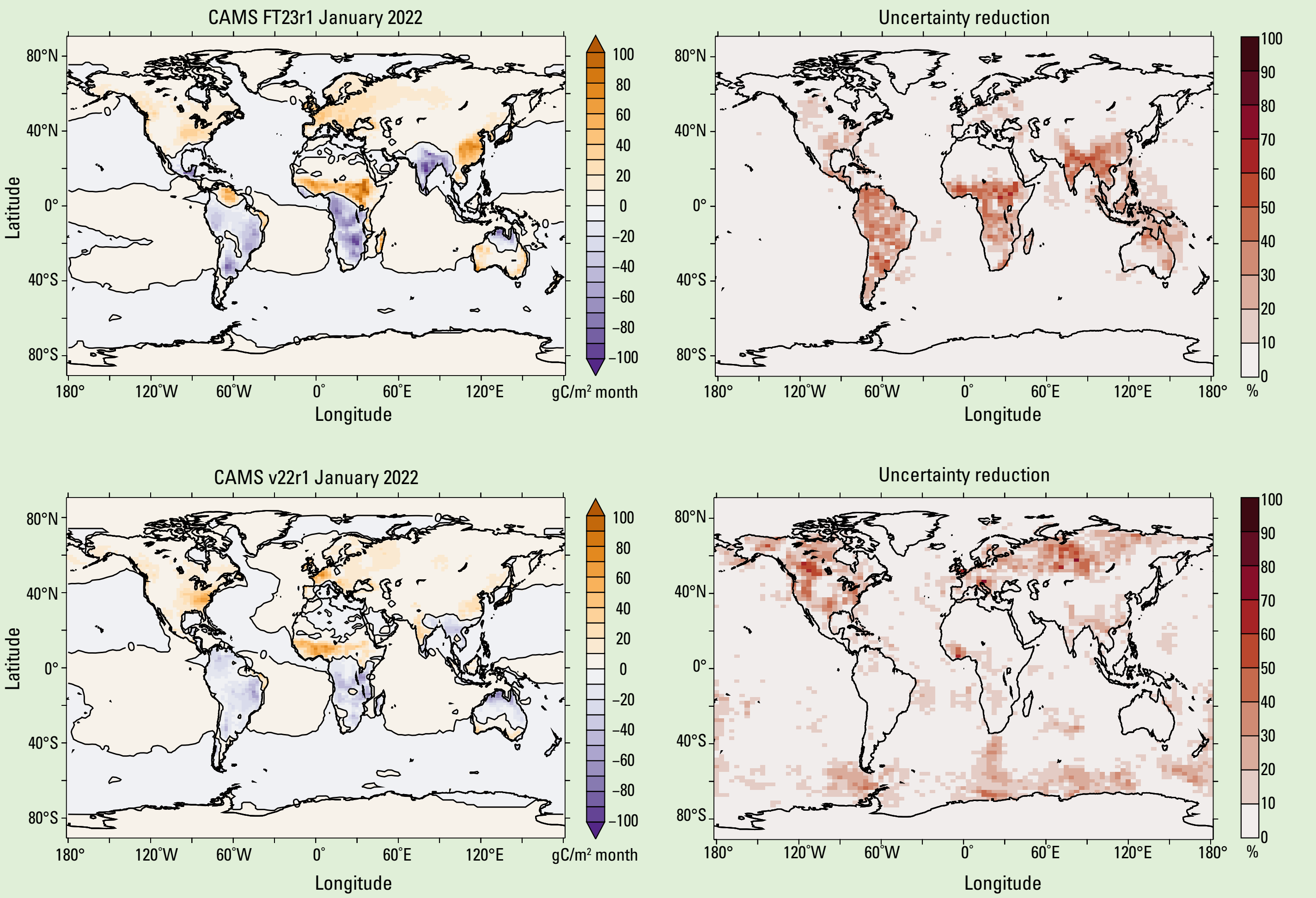

Figure 9. Example result for monthly fluxes for January 2022 from the Copernicus Atmosphere Monitoring Service (CAMS) inversion system [14], one of the 14 atmospheric inversion systems used in the Global Carbon Project 2023. The top panels show the result for an inversion using OCO-2 satellite information only. The bottom panels show the result using surface observations only. The left plot is always the optimized flux for land ecosystem plus ocean flux of CO_2. The right plot is the uncertainty reduction compared to the initial estimated uncertainty of the flux in the respective inversion due to the use of observations.

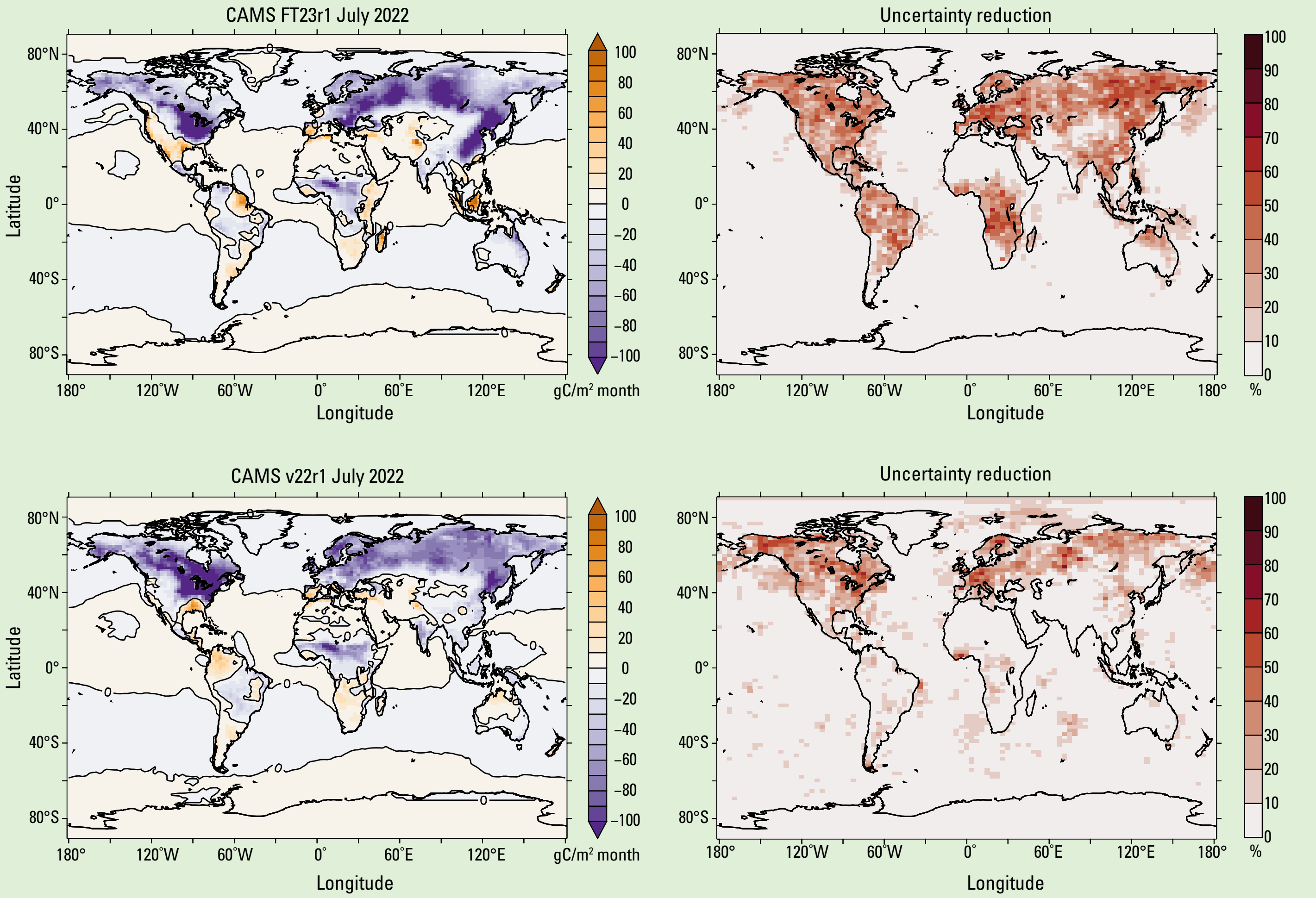

Figure 10. Example result for monthly fluxes for July 2022 from the Copernicus Atmosphere Monitoring Service (CAMS) inversion system [14], one of the 14 atmospheric inversion systems used in the Global Carbon Project 2023. The top panels show the result for an inversion using OCO-2 satellite information only. The bottom panels show the result using surface observations only. The left plot is always the optimized flux for land ecosystem plus ocean flux of CO_2. The right plot is the uncertainty reduction compared to the initial estimated uncertainty of the flux in the respective inversion due to the use of observations.

estimates, we can point out where and how improvements are needed to better inform us of the state of the GHG budget of the planet.

GGGW will require additional, strategically placed observations of sufficient accuracy in undersampled regions such as Africa, South America, the Arctic and the oceans, together with multiple coordinated data centres to process and analyse the data and open and transparent data sharing mechanisms for all data and methods. The WMO GAW network and its decades-long development of guidelines and methodology for quality assurance and control, as applied in the GAW network and contributing networks, such as the Advanced Global Atmospheric Gases Experiment (AGAGE), the Integrated Carbon Observation System (ICOS) and NOAA, form a solid basis for the expansion towards a sustained, long-term, operational observational network central to GGGW. Recent developments in inverse modelling-based surface flux calculations allow analysis of GHG signals with minimal delays [15].

In addition to atmospheric concentration measurements, the isotopic composition of GHGs and ancillary useful tracers such as COS and atmospheric O_2, an extensive set of additional space-based and surface-based observations will be needed to determine GHG exchanges from ocean and land ecosystems and urban regions. Additionally, GGGW will need to identify and develop sets of well-calibrated GHG observations that can be withheld from the inversion modelling process for cross-validation. Analyses of the degree to which inversion models can represent these independent data can be used to help quantify, understand, and eventually minimize random and systematic errors within inverse modelling systems.

to 2021 and higher than the average annual increase of 10.2 ppb over the past decade. The mean annual increase of CH_4 decreased from approximately 12 ppb yr^{-1} during the late 1980s to near zero during 1999–2006. Since 2007, atmospheric CH_4 has again been increasing. It was 264% of the pre-industrial level in 2022, driven by anthropogenic sources. It is critical to remember that unlike the case with CO_2, CH_4 anthropogenic sources are not predominately driven by fossil fuel-related emissions; agricultural sources also play a significant role. Studies using GAW CH_4 measurements indicate that increased CH_4 emissions from wetlands in the tropics and from anthropogenic sources at the mid-latitudes of the northern hemisphere are the likely causes of this recent increase (see WMO Greenhouse Gas Bulletin No. 18).

Nitrous Oxide (N_2O)

Nitrous oxide accounts for about 6%[(4)] of the radiative forcing by LLGHGs. It is the third most important individual contributor to the combined forcing. N_2O is emitted into the atmosphere from both natural sources (approximately 57%) and anthropogenic sources (approximately 43%), including oceans, soils, biomass burning, fertilizer use, and various industrial processes.

The globally averaged N_2O concentration in 2022 reached 335.8 ±0.1 ppb, which is an increase of 1.4 ppb with respect to the previous year (Figure 7) and 124% of the pre-industrial level (270.1 ppb). The annual increase from 2021 to 2022 was higher than the increase from 2020 to 2021 and higher than the mean growth rate over the past 10 years (1.05 ppb yr^{-1}). Global human-induced N_2O emissions, which are dominated by nitrogen additions to croplands, increased by 30% over the past four decades to 7.3 (range: 4.2–11.4) teragrams of nitrogen per year. This increase was mainly responsible for the growth in the atmospheric burden of N_2O [11]. A continued La Niña over the period 2020–2022 could have played a role in causing the N_2O growth rate to be so elevated.

Other greenhouse gases

Stratospheric ozone-depleting chlorofluorocarbons (CFCs), for example the ones depicted in Figure 8, which are regulated by the Montreal Protocol on Substances that Deplete the Ozone Layer, together with minor halogenated gases, account for approximately 11%[(4)] of the radiative forcing by LLGHGs. While CFCs and most halons are decreasing, some hydrochlorofluorocarbons

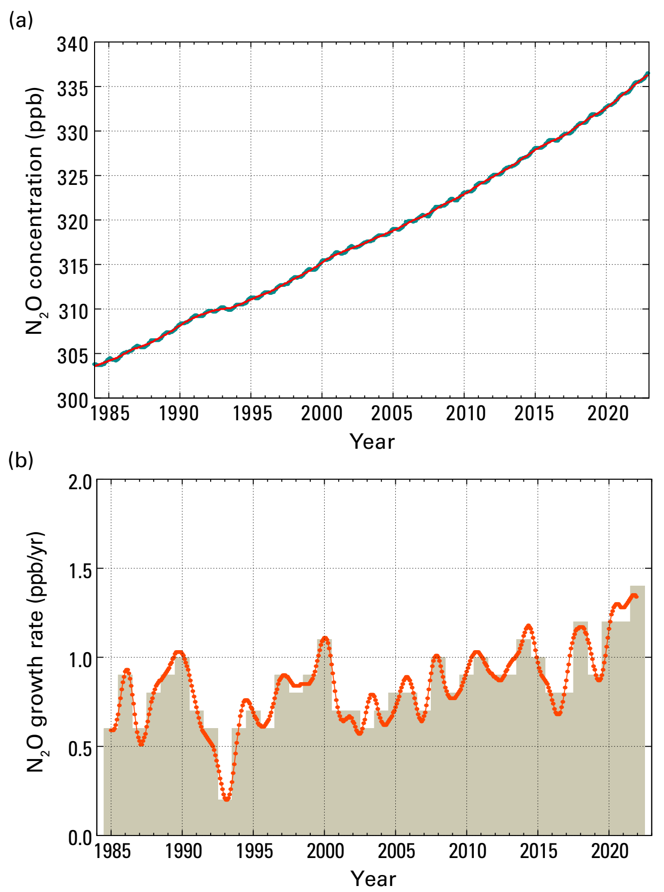

Figure 7. Globally averaged N_2O concentration (a) and its growth rate (b) from 1984 to 2022. Increases in successive annual means are shown as the shaded columns in (b). The red line in (a) is the monthly mean with the seasonal variation removed; in this plot, the red line overlaps the blue dots and blue line that depict the monthly averages. Observations from 109 stations were used for this analysis.

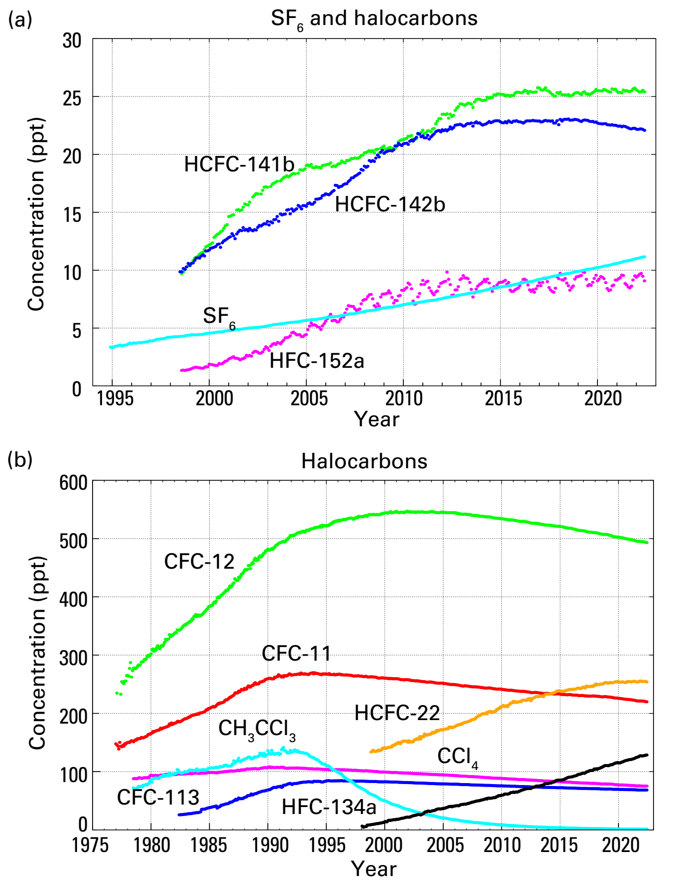

Figure 8. Monthly mean concentration of sulfur hexafluoride (SF_6) and the most important halocarbons: (a) SF_6 and lower halocarbon concentrations and (b) higher halocarbon concentrations. For each gas, the number of stations used for the analysis was as follows: SF_6 (88), CFC-11 (24), CFC-12 (26), CFC-113 (22), CCl_4 (23), CH_3CCl_3 (25), HCFC-141b (11), HCFC-142b (15), HCFC-22 (15), HFC-134a (12), HFC-152a (11).

(HCFCs) and hydrofluorocarbons (HFCs), which are also potent greenhouse gases, are increasing at relatively rapid rates; however, they are still low in abundance (at ppt[6] levels). Although at a similarly low abundance, sulfur hexafluoride (SF_6) is an extremely potent LLGHG. It is produced by the chemical industry, mainly as an electrical insulator in power distribution equipment. Its concentration is rising at a quite constant rate and is now more than twice the level observed in the mid-1990s (Figure 8(a)).

The present Bulletin primarily addresses long-lived greenhouse gases. Relatively short-lived tropospheric ozone [12] has a radiative forcing comparable to that of the halocarbons; because of its short lifetime, its horizontal and vertical variability is very high, and global means are not well characterized with a network such as that shown in Figure 3. Many other pollutants, such as carbon monoxide, nitrogen oxides and volatile organic compounds, although not referred to as greenhouse gases, have small direct or indirect effects on radiative forcing [16]. Aerosols (suspended particulate matter) are short-lived substances that alter the radiation budget. All the gases mentioned in the present Bulletin, as well as aerosols, are included in the observational programme of GAW, with support from WMO Members and contributing networks.

Notes:

(1) The scientifically correct term for the abundance in the atmosphere of compounds such as carbon dioxide and other (greenhouse) gases is dry air **mole fraction**, expressed as the number of moles of each gas per mole of dry air, often with units of ppm[2] or ppb[3]. However, in the GHG Bulletin, we use the more popular term **concentration** to avoid possible confusion for the public.

(2) ppm – the number of molecules of a gas per million (10^6) molecules of dry air

(3) ppb – the number of molecules of a gas per billion (10^9) molecules of dry air

(4) This percentage is calculated as the relative contribution of the mentioned gas(es) to the increase in global radiative forcing caused by all long-lived greenhouse gases since 1750. Radiative forcing is the perturbation to the Earth's energy budget resulting from the increased burdens of greenhouse gases since the pre-industrial (1750) period after allowing stratospheric temperature to quickly adjust. "Effective" radiative forcing also includes fast tropospheric adjustments. Note that the numbers presented here account only for the direct radiative forcing of CH_4 and CO_2, as opposed to the emission-based forcings used in the IPCC AR6 WG1 report, which include estimated indirect forcings due the atmospheric chemistry of CH_4, influencing other atmospheric constituents.

(5) 1 Gt CO_2 = 1 billion (10^9) metric tons of carbon dioxide

(6) ppt – the number of molecules of the gas per trillion (10^{12}) molecules of dry air

Acknowledgements and links

Fifty-five WMO Members contributed CO_2 and other greenhouse gas data to the GAW WDCGG. Approximately 47% of the measurement records submitted to WDCGG were obtained at sites of the NOAA Global Monitoring Laboratory cooperative air-sampling network. For other networks and stations, see [13]. The Advanced Global Atmospheric Gases Experiment also contributed observations to the present Bulletin. The GAW observational stations that contributed data to the present Bulletin, shown in Figure 3, are included in the list of contributors on the WDCGG web page. They are also described in the GAW Station Information System (GAWSIS), supported by MeteoSwiss, Switzerland. The present Bulletin has been prepared under the oversight of the GAW Scientific Advisory Group on Greenhouse Gases.

Editorial team

Alex Vermeulen (Integrated Carbon Observation System – European Research Infrastructure Consortium (ICOS ERIC)/Lund University, Sweden), Oksana Tarasova (WMO), Yousuke Sawa (Japan Meteorological Agency, WDCGG, Japan)

Authors (in alphabetical order)

Frederic Chevallier (Laboratoire des Sciences du Climat et de l'Environnement (LSCE), Paris, France), Andrew Crotwell (NOAA Global Monitoring Laboratory and Cooperative Institute for Research in Environmental Sciences, University of Colorado Boulder, United States of America), Christoph Gerbig (Max Planck Institute for Biogeochemistry, Germany), Armin Jordan (Max Planck Institute for Biogeochemistry, Germany), Xin Lan (NOAA Global Monitoring Laboratory, USA), Zoë Loh (Commonwealth Scientific and Industrial Research Organisation, Australia), Ingrid Luijkx (Wageningen University and Research, Netherlands), John Miller (NOAA Global Monitoring Laboratory, USA), Yousuke Sawa (Japan Meteorological Agency, WDCGG, Japan), Oksana Tarasova (WMO), Alex Vermeulen (ICOS ERIC/ Lund University, Sweden), Ray Weiss (Scripps Institution of Oceanography, University of California San Diego, USA), Thorsten Warneke (University Bremen, Germany), Camille Yver (LSCE, Paris, France)

References

[1] van der Woude, A. M.; Peters, W.; Joetzjer, E. et al. Temperature Extremes of 2022 Reduced Carbon Uptake by Forests in Europe. *Nature Communications* **2023**, *14* (1), 6218. https://doi.org/10.1038/s41467-023-41851-0.

[2] Wu, Z.; Vermeulen, A.; Sawa, Y. et al. Investigating the Differences in Calculating Global Mean Surface CO_2 Abundance: The Impact of Analysis Methodologies and Site Selection. *EGUsphere* **2023** [preprint]. https://doi.org/10.5194/egusphere-2023-1173.

[3] Friedlingstein, P.; O'Sullivan, M.; Jones, M. W. et al. Global Carbon Budget 2022. *Earth System Science Data* **2022**, *14* (11), 4811–4900. https://doi.org/10.5194/essd-14-4811-2022.

[4] National Oceanic and Atmospheric Administration (NOAA) Earth System Research Laboratories Global Monitoring Laboratory. *CarbonTracker CT2022*. https://gml.noaa.gov/ccgg/carbontracker/.

[5] Montzka, S. A. *The NOAA Annual Greenhouse Gas Index (AGGI)*; National Oceanic and Atmospheric Administration (NOAA) Earth System Research Laboratories Global Monitoring Laboratory, 2023. http://www.esrl.noaa.gov/gmd/aggi/aggi.html.

[6] National Oceanic and Atmospheric Administratin (NOAA) Earth System Research Laboratories Global Monitoring Laboratory. *Trends in Atmospheric Carbon Dioxide*. 2023. http://www.esrl.noaa.gov/gmd/ccgg/trends/.

[7] Tsutsumi, Y.; Mori, K.; Hirahara, T. et al. *Technical Report of Global Analysis Method for Major Greenhouse Gases by the World Data Center for Greenhouse Gases* (WMO/TD-No. 1473). GAW Report No. 184. World Meteorological Organization (WMO): Geneva, 2009.

[8] Hall, B. D.; Crotwell, A. M.; Kitzis, D. R. et al. Revision of the World Meteorological Organization Global Atmosphere Watch (WMO/GAW) CO_2 Calibration Scale. *Atmospheric Measurement Techniques* **2021**, *14* (4), 3015–3032. https://doi.org/10.5194/amt-14-3015-2021.

[9] International Energy Agency (IEA). *CO_2 Emissions in 2022*; IEA: Paris, 2023. https://www.iea.org/reports/co2-emissions-in-2022

[10] Saunois, M.; Stavert, A. R.; Poulter, B. et al. The Global Methane Budget 2000–2017. *Earth System Science Data* **2020**, 12 (3), 1561–1623. https://doi.org/10.5194/essd-12-1561-2020.

[11] Tian, H.; Xu, R.; Canadell, J. G. et al. A Comprehensive Quantification of Global Nitrous Oxide Sources and Sinks. *Nature* **2020**, 586 (7828), 248–256. https://doi.org/10.1038/s41586-020-2780-0.

[12] World Meteorological Organization (WMO). *WMO Reactive Gases Bulletin, No. 2: Highlights from the Global Atmosphere Watch Programme*; WMO: Geneva, 2018.

[13] World Meteorological Organization (WMO). 20th WMO/IAEA Meeting on Carbon Dioxide, Other Greenhouse Gases and Related Measurement Techniques (GGMT-2019). GAW Report No. 255. WMO: Geneva, 2020.

[14] Chevallier, F.; Lloret, Z.; Cozic, A. et al. Toward High-Resolution Global Atmospheric Inverse Modeling Using Graphics Accelerators. *Geophysical Research Letters* **2023**, 50 (5), e2022GL102135. https://doi.org/10.1029/2022GL102135.

[15] van der Woude, A. M.; de Kok, R.; Smith, N. et al. Near-Real-Time CO_2 Fluxes from CarbonTracker Europe for High-Resolution Atmospheric Modeling. *Earth System Science Data* **2023**, *15* (2), 579–605. https://doi.org/10.5194/essd-15-579-2023.

[16] Intergovernmental Panel on Climate Change (IPCC). Summary for Policymakers. In *Climate Change 2021: The Physical Science Basis. Contribution of Working Group I to the Sixth Assessment Report of the Intergovernmental Panel on Climate Change*. Masson-Delmotte, V.; Zhai, P.; Pirani, A. et al. Eds.; Cambridge University Press: Cambridge, UK and New York, USA, 2021. https://www.ipcc.ch/report/ar6/wg1/downloads/report/IPCC_AR6_WGI_SPM.pdf.

SELECTED GREENHOUSE GAS OBSERVATORIES

Ulleungdo (ULD), South Korea

The Ulleungdo (ULD) station, operated by the National Institute of Meteorological Sciences (NIMS) of the Korea Meteorological Administration since 2014, became a GAW regional station in September 2023. It is located on Ulleungdo Island, which lies approximately 155 km east of the Korean Peninsula at 37.48°N, 130.90°E. The island is 220.9 meters above sea level and has an area of 72.86 km^2. The measurement programme at the ULD station includes observations of GHGs such as CO_2, CH_4, N_2O, and SF_6, as well as reactive gases such as CO, aerosols, ultraviolet radiation, and wet deposition. The station plays a pivotal role as a key observational site, facilitating comprehensive data collection from air originating across East Asia.

Overview of the Ulleungdo station
Photo: Korea Meteorological Administration

Location

Country: Republic of Korea

Latitude: 37.4800°N

Longitude: 130.9000°E

Elevation: 220.9 m asl

Time zone: UTC+9

WMO Integrated Global Observing System (WIGOS) ID: 0-410-0-ULD

GAW trigram: ULD

Mauna Loa Observatory (MLO) update

NOAA's Mauna Loa Observatory (MLO) is located on the north flank of Mauna Loa volcano, on the island of Hawaii, at an elevation of 3 397 meters above sea level. Modern and well-calibrated atmospheric CO_2 measurements were started at this site by Charles David Keeling, a geoscientist from Scripps Institution of Oceanography (SIO), in 1958. On 29 November 2022, operations at Mauna Loa Observatory stopped due to the eruption of the Mauna Loa volcano, when lava flow crossed the access road and took out power lines to the facility. After a 10-day interruption, NOAA started greenhouse gas observations from a temporary station located near the summit of Mauna Kea, a dormant volcano located approximately 33 km north of Mauna Loa. SIO initiated air sampling at Mauna Kea Observatory (MKO) a week later and resumed CO_2 sampling at MLO in March 2023. NOAA resumed its flask-air GHG sampling at MLO on 21 December 2022 via helicopter, while NOAA's in-situ CO_2 analyser resumed sampling in July 2023. As of October 2023, the observatory remains inaccessible by on-road vehicles. Power is not available from the local utility company; the observatory is running on a limited amount of solar power.

While the MLO CO_2 record is useful for monitoring the average state of atmospheric CO_2, we need a network of CO_2 measurements to understand regional CO_2 emissions and terrestrial and oceanic processes that are driving regional and global changes. A sufficiently large measurement network also provides the insurance of continuity when an unexpected interruption occurs.

Overview of the Mauna Loa Observatory
Photo: Brian Vasel

Lava covering the access road to the NOAA Mauna Loa Baseline Observatory during the 2022 Mauna Loa eruption
Photo: NOAA

Location
Country: USA
Latitude: 19.53623°N
Longitude: 155.57616°W
Elevation: 3 397 m asl
Time zone: UTC-10
WIGOS ID: 0-20008-0-MLO
GAW trigram: MLO

Contacts

World Meteorological Organization
Atmospheric Environment Research Division,
Science and Innovation Department, Geneva
Email: gaw@wmo.int
Website: https://community.wmo.int/activity-areas/gaw

World Data Centre for Greenhouse Gases
Japan Meteorological Agency, Tokyo
Email: wdcgg@met.kishou.go.jp
Website: https://gaw.kishou.go.jp

JN 231327